

Christopoulou, Eleftheria-Panagiota & Zervas Konstantinos
Department of Physics , University of Patras, Greece

Examining a PCEB system's planetary neighbours

NSVS 14256825: a PCEB with 2 possible exoplanets

PCEB name	PCEB type	NEA	EPA	REF	Stability	Reference
Kepler-451	sdB+dM	3	3	3	unstable	Esmer et al. (2022)
HW Vir	sdB+dM	-	-	3	unstable	Mai & Mutel (2022)
NN Ser	WD+dM	2	2	2	stable	Marsh et al. (2014)
NY Vir	sdB+dM	2	2	2	stable	Esmer et al. (2023)
V470 Cam	sdB+dM	-	-	1	-	Mai & Mutel (2022)
NSVS 14256825	sdB+dM	1	-	1	-	Pulley et al. (2022)
DE CVn	WD+dM	1	-	1	-	Han et al. (2018)
RR Cae	WD+dM	1	1	1-2	-	Rattanamala et al. (2023)
OGLE-GD-ECL-11388	sdB+dM	-	1	1	-	Hong et al. (2016)
KIC 10544976	WD+dM	-	-	1	-	Almeida et al. (2019)
V471 Tau	WD+dM	-	-	1	-	Kundra et al. (2022)
SDSS J1435+3733 Boo	WD+dM	-	-	1	-	Wolf et al. (2021)
NSVS 07826147	sdB+dM	-	-	1	-	Wolf et al. (2021)

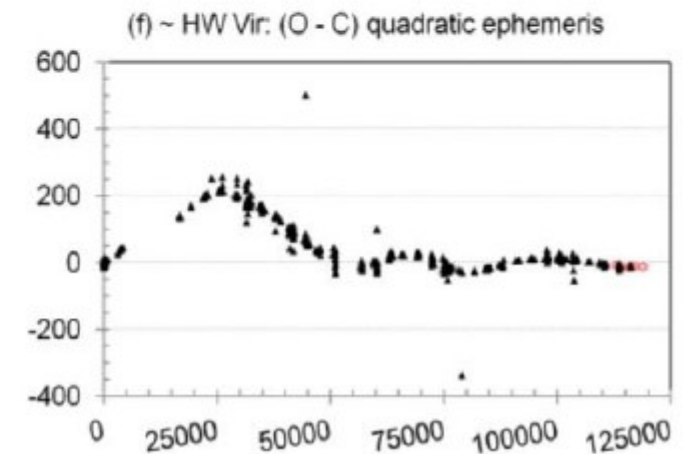
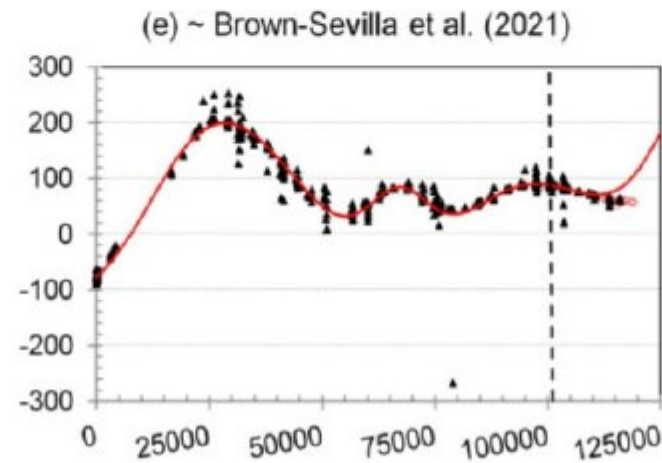
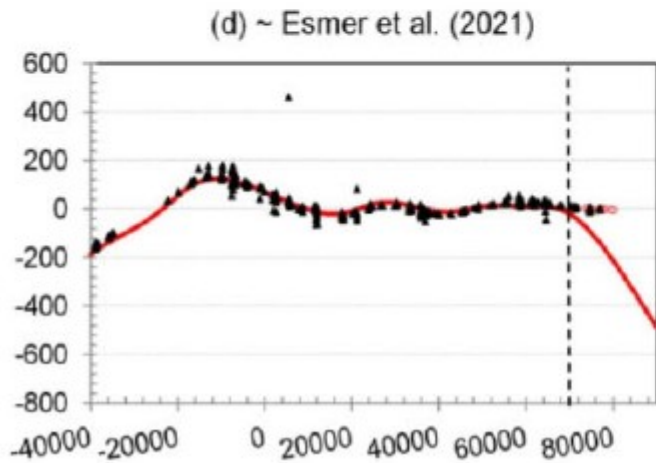
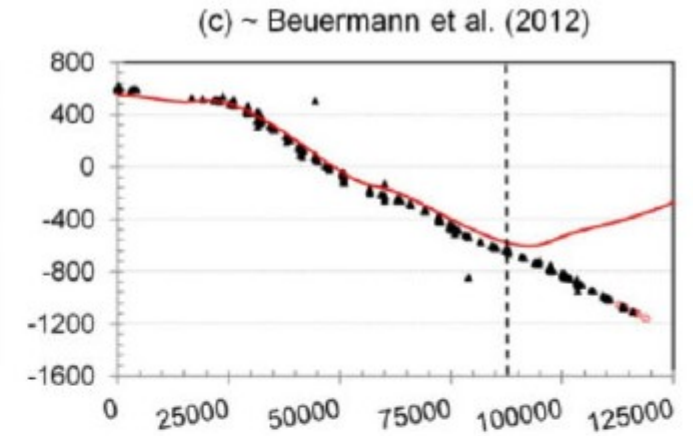
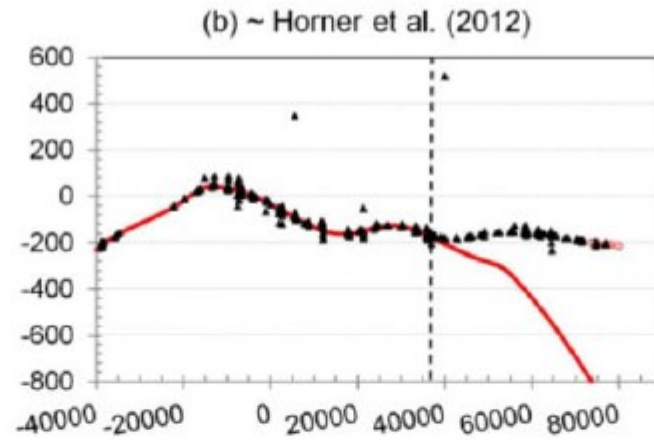
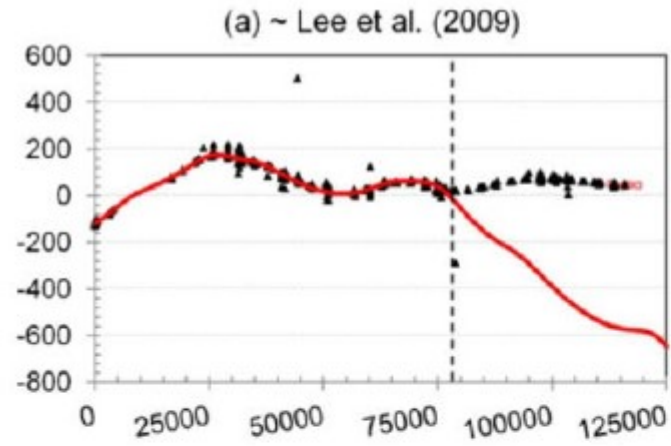
- PCEBs with giant circumbinary planets through ETVs (Zorotovic & Schreiber 2013; Heber 2016) caused by the light-travel time effect (LTTE) (Irwin 1952; Borkovits et al. 2015)
- 10 PCEBs circumbinary brown dwarfs or planets (Marsh 2018)

NEA: 5600+ exoplanets (various methods)
 508 in multiple stars
 441 in binary stars: **17 ETV detections**
11 ETV in 6 PCEBs

REF: **19 ETV in 13 PCEBs**

NEA: Nasa Exoplanets Archive
 EPA: Extrasolar Planets Encyclopedia
 REF: Reference of publication

Pulley et al. 2022 20 yrs HS0705 + 6700 , HW Vir, NN Ser, NY Vir, NSVS 14256825, RR Cae, DE CVn



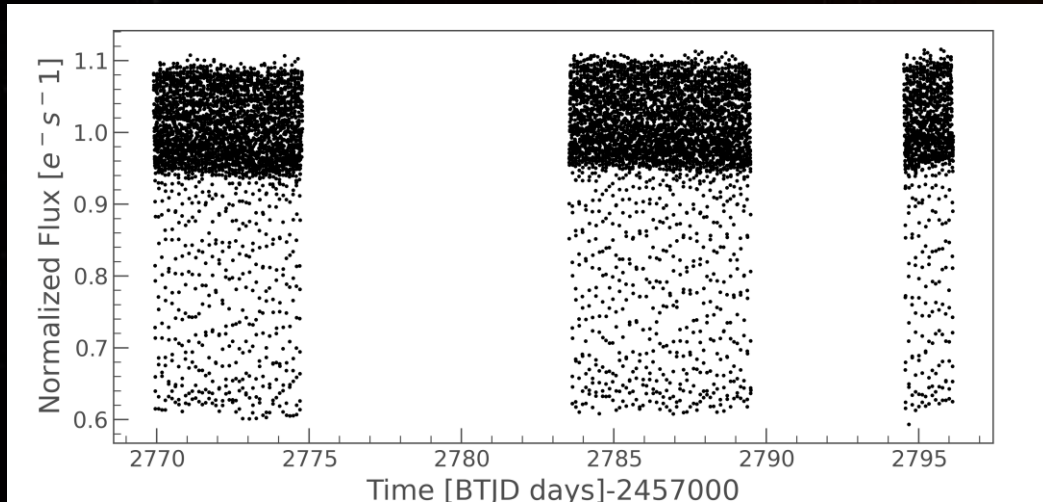
Mai & Mutel 2022

NSVS 14256825: the profile

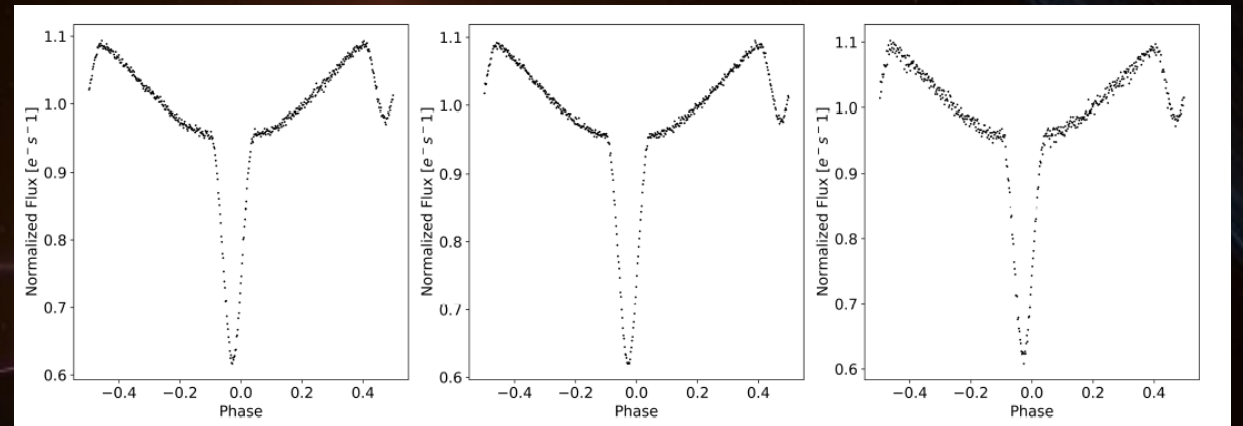
- Northern Sky Variability Survey : 13.2 mag (Woźniak et al. 2004), $\Delta V \sim 0.8 \text{ mag}$ (Wils et al. 2007)
- $P = 0.1104 \text{ d} = 2.65 \text{ hr}$
- PCEB: sdOB+dM Almeida et al. (2012) - Nehir & Bulut (2022)
 - $i = 82^\circ.5 \pm 0^\circ.3, q = 0.260 \pm 0.012$
 - $M_1 = 0.419 \pm 0.070 M_\odot, M_2 = 0.109 \pm 0.023 M_\odot$
 - $R_1 = 0.188 \pm 0.010 R_\odot, R_2 = 0.162 \pm 0.008 R_\odot$
 - $T_1 = 42000 \pm 400 \text{ K}, T_2 = 2550 \pm 550 \text{ K}$

Reference	e_b	P_b (yr)	M_b (M_{Jup})	e_c	P_c (yr)	M_c (M_{Jup})
Beuermann et al. (2012)	0.5	20	12	-	-	-
Almeida et al. (2013)	0.0	6.9	2.9	0.52	6.9	8.1
Wittenmyer et al. (2013)	N body proved unstable configuration					
Nasiroglu et al. (2017)	0.18	9.9	15	-	-	-
Zhu et al. (2019)	0.12	8.8	14.2	-	-	-
Nehir & Bulut (2022)	0.13	8.83	13.2	-	-	-
Wolf et al. (2021)	-	14	-1 LITE insufficient to explain the updated ETV data 2007-2021			
Pulley et al. (2022)	0.02	7.7				

Long and conflicting ETV history (6 models)



TESS LC time series 2 min cadence (sector 51) 2022
(Zervas et al . 2024ApJ...961...97Z)



generated phase-folded binned LCs for each 1/3 segment

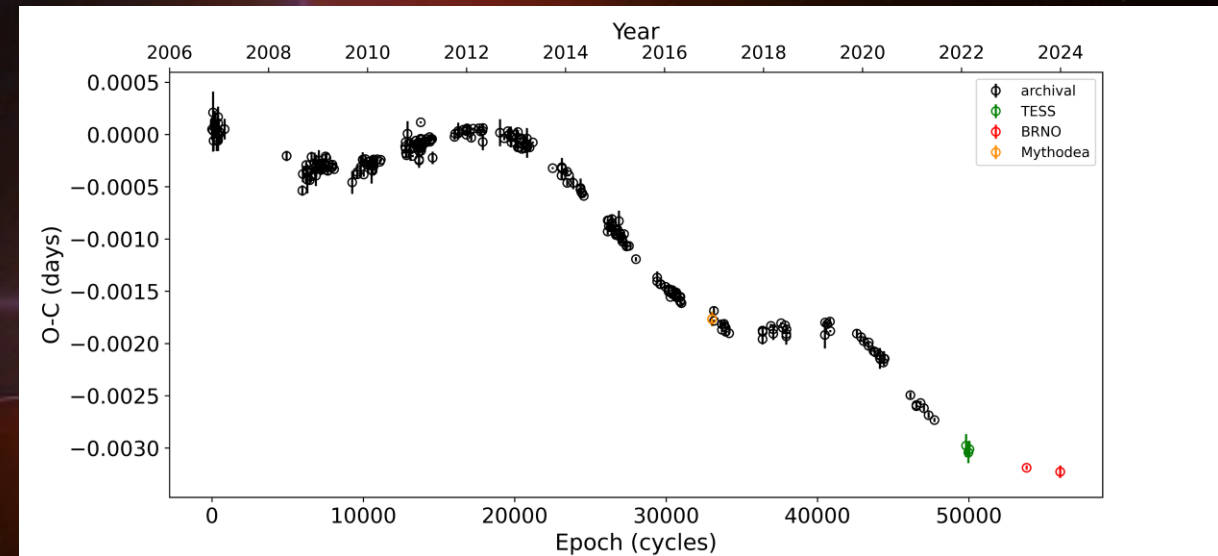
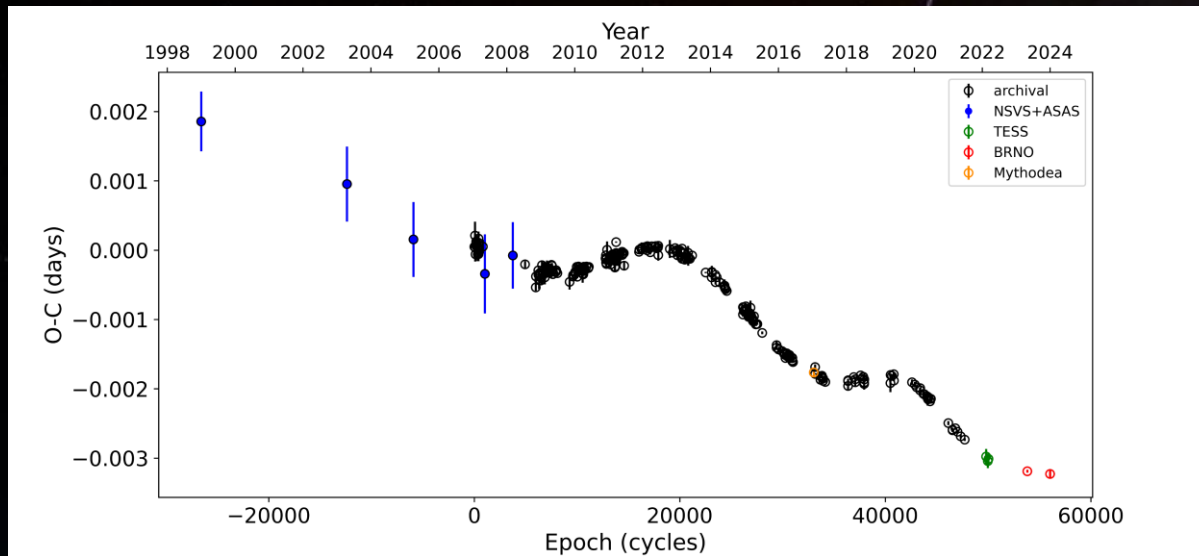
BJD-240000 (d)	Epoch (cycles)	O-C (d)	Error (d)	Source
57919.47908	33026.5	-0.00177	0.00007	Mythodea
57919.53427	33027.0	-0.00176	0.00007	Mythodea
59771.05954	49802.0	-0.00298	0.00011	TESS
59789.27121	49967.0	-0.00304	0.00010	TESS
59796.11444	50029.0	-0.00301	0.00008	TESS
60213.43895	53810.0	-0.00319	0.00002	B.R.N.O.
60458.46954	56030.0	-0.00323	0.00006	B.R.N.O.

NSVS 14256825: ETV diagram

Dataset A (1999-2024); 312 TOMs with $\sigma < 17\text{sec}$ (0.0002 d)
305 from literature
Mythodea: (2017); 2 TOMs
TESS: (2022); 3 TOMs
BRNO: (2023, 2024); 2 TOMs

Dataset B (2007-2024); 307 TOMs, $\sigma < 17\text{sec}$ (0.0002 d)
excluding NSVS+ASAS: (1999-2008); 5 TOMs

$$BJD = 2454274.20875(5) + 0.110374157(4)E \quad \text{Pulley et al. (2022)}$$



NSVS 14256825: ETV Analysis Outline

$$LTTE_p = K_p \left[\sin \omega_p \cos(E_p(t) - e_p) + \cos \omega_p \sqrt{1 - e_p^2} \sin E_p(t) \right]$$

Goździewski et al. (2012)

“Revised Keplerian formulation of the LTTE effect (Irwin 1952) for multiple circumbinary companions by expressing eclipse ephemerides w.r.t. Jacobi coordinates with the origin at the CM of the binary”

K_p the semi-amplitude of the LTTE signal
 e_p the eccentricity
 ω_p the argument of the pericenter
 $E_p(t)$ eccentric anomaly (P_p, T_p)
 for body p ($p = b$ for inner orbit, $p = c$ for outer orbit).

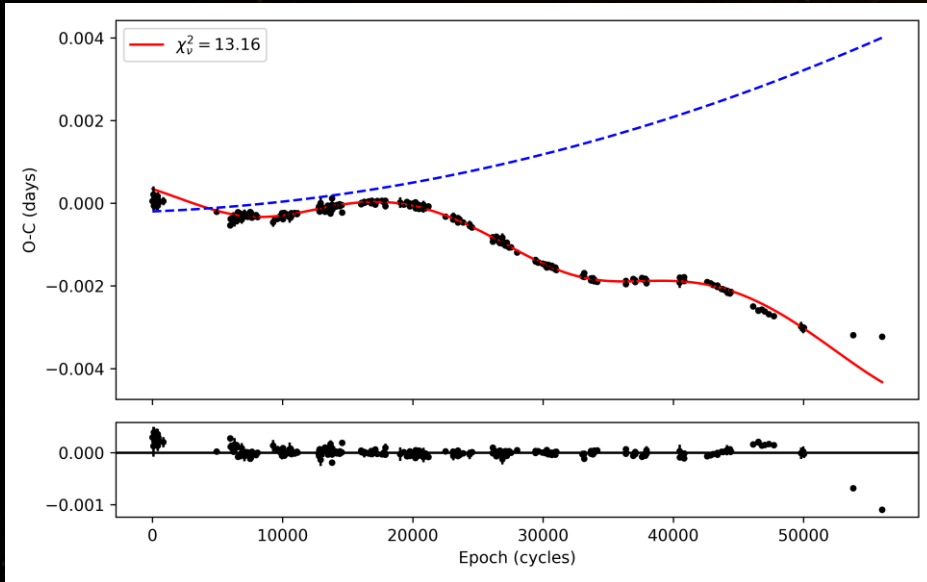
$$\text{LSF} \quad \chi^2 = \sum_{i=1}^N \left(\frac{(D_{O-C} - M_{O-C})_i}{\sigma_i} \right)^2$$

12 Parameters 2 for the linear Ephemeris T_0, P_{bin}
 5×2 $p = b, c$

$$M_{O-C} = \sum_{i=0}^2 c_i E^i + M_{effect}$$

$\alpha_p \sin i_p$
 e_p
 P_p
 ω_p
 T_p

NSVS 14256825: ETV Analysis Outline



1 LTTE + QMT fit

Acceptable model:
Good fit to the data and is secularly stable with non-chaotic orbital behavior.

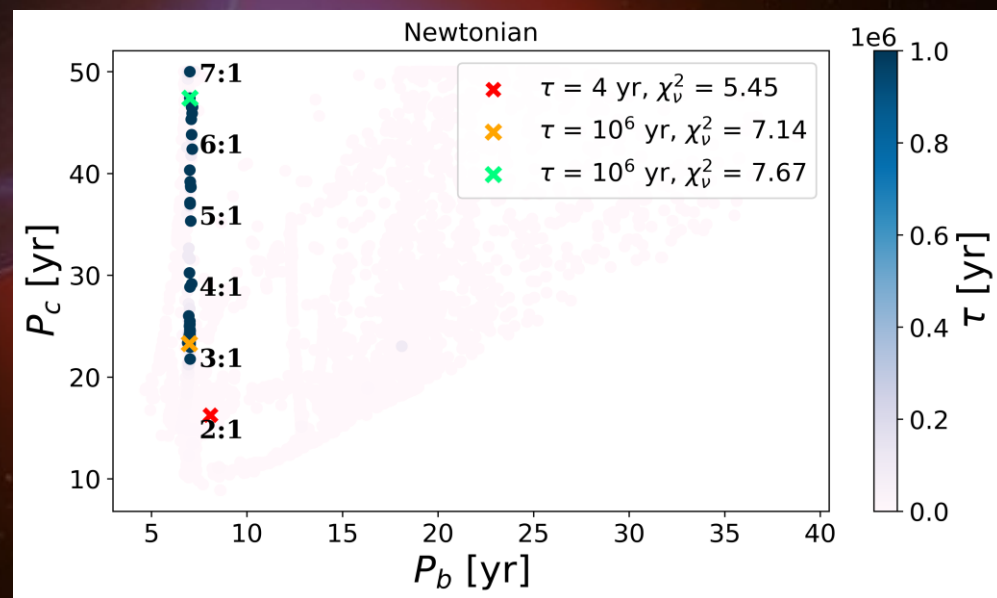
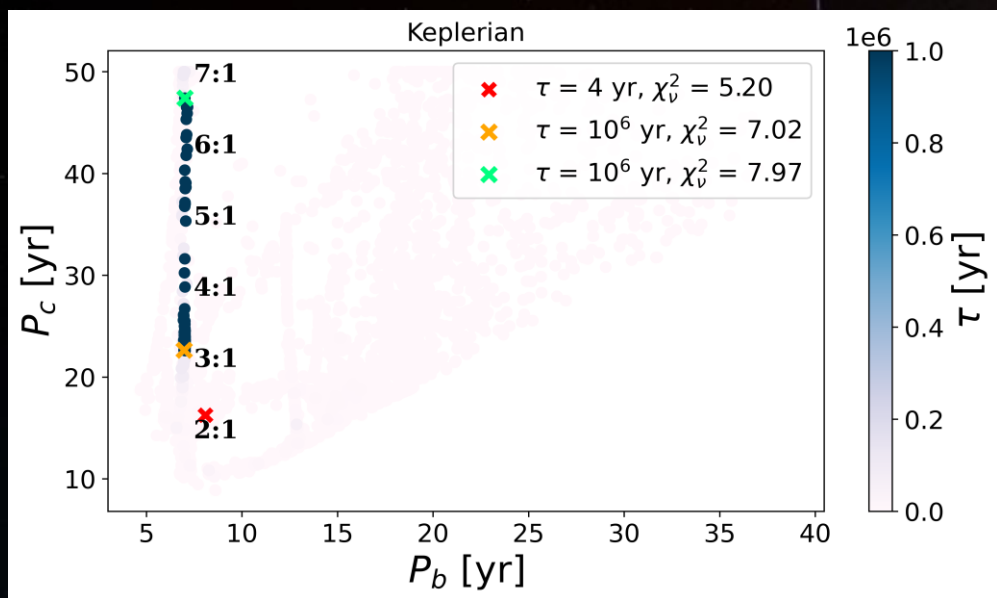
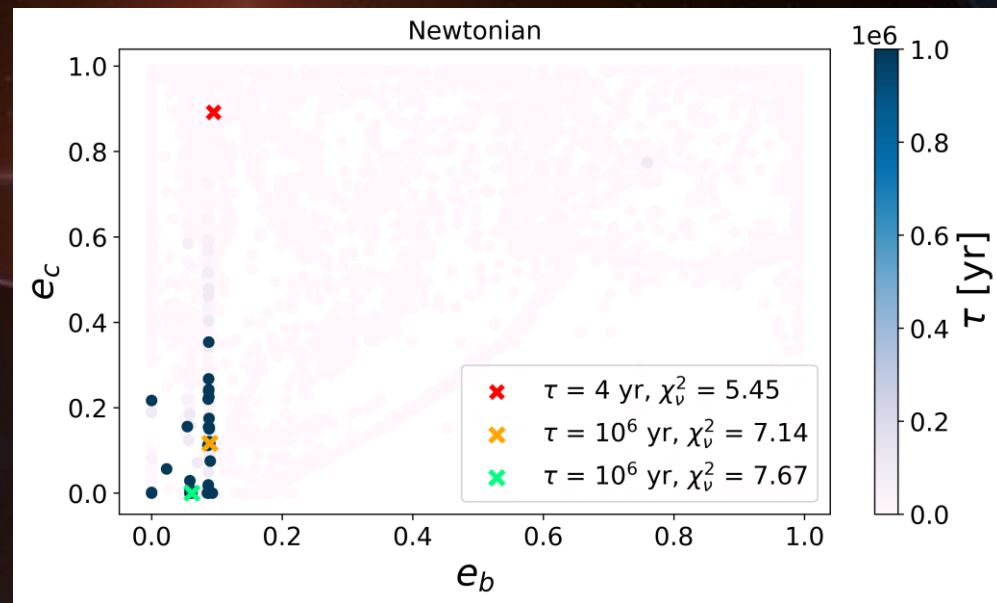
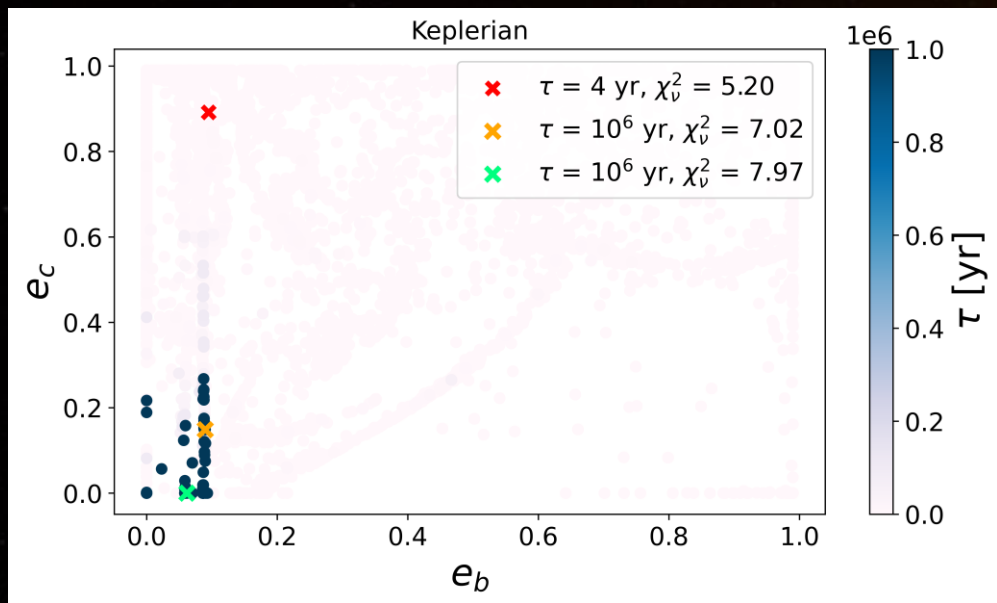
Grid search approach (Beurmann et al. 2013) 2 LTTE terms
Our optimization process

1. Run 1: Nelder-Mead Simplex and Levenberg-Marquardt grid search in e_b, e_c plane with fixed values: $[0.0, 0.98]$, 0.01 step \rightarrow 9801 models e_b, e_c fixed
2. Run 2: adjust results of Run 1 (LMFIT Python package (Newville et al. 2023))
3. Each Keplerian solution of both runs that lie in the 90% conf. level of the $\chi_{v,best}^2$: $\chi_v^2 \leq \chi_{v,best}^2 + 4.6$ was integrated with the REBOUND N-body code for 1 Myr and chaotic indicator value MEGNO $\langle Y \rangle \sim 2$
4. Self-consistent N-body (Newtonian) fits initialized from each Keplerian fit of step 3 and integration for 1 Myr.

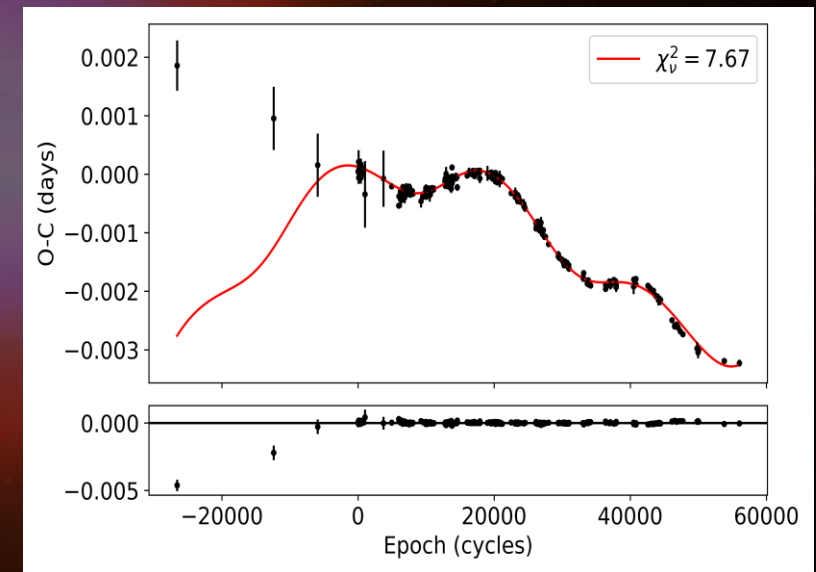
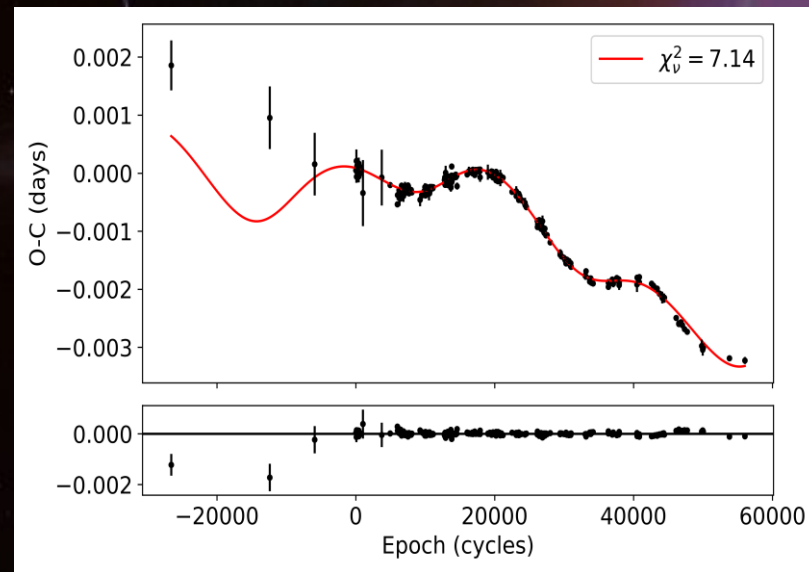
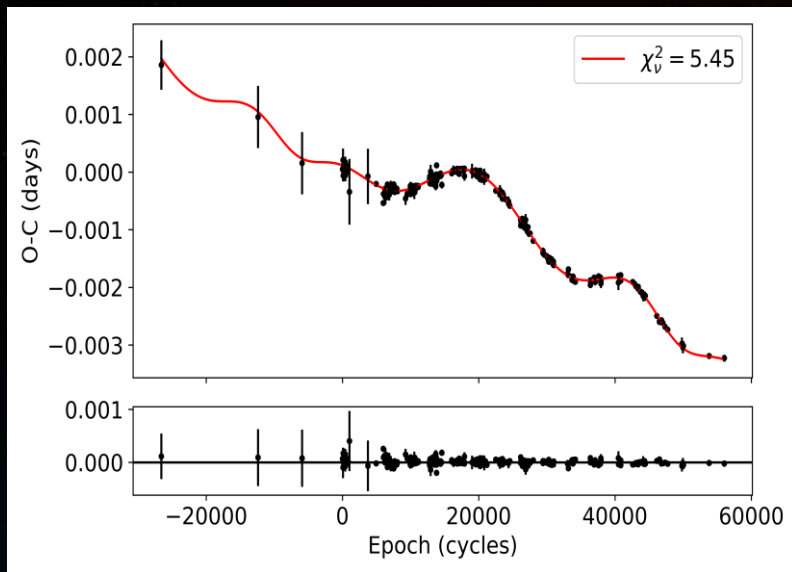
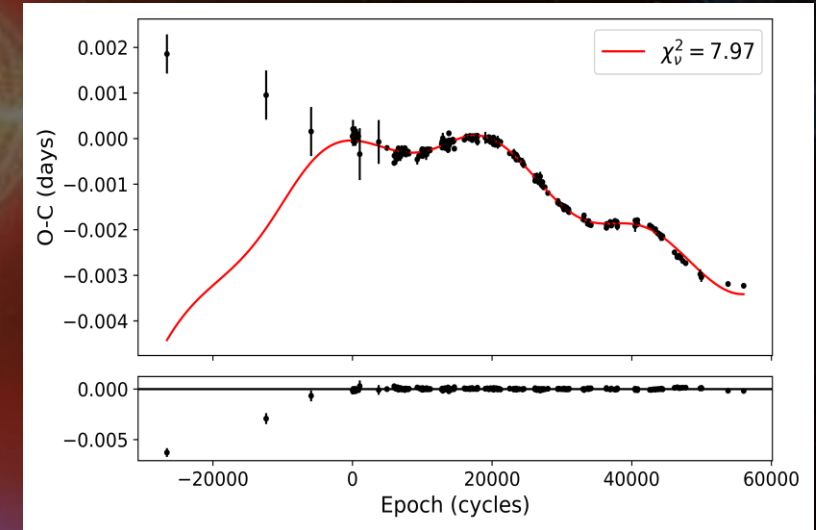
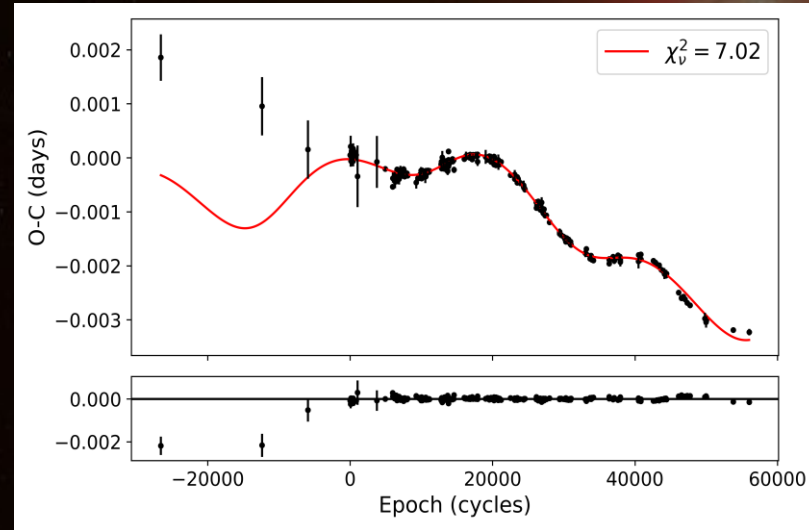
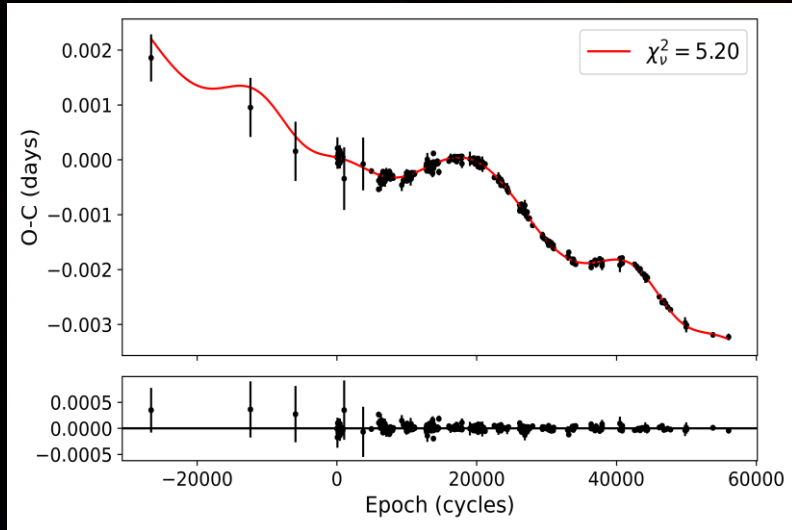
We treated the central binary as a single object throughout all orbital simulations and considered only co-planar, edge-on cases.

NSVS 14256825: Dataset A (Run 2) - lifetime distributions (colormaps)

153 stable Keplerian orbits and 93 stable Newtonian orbits (8123 models)

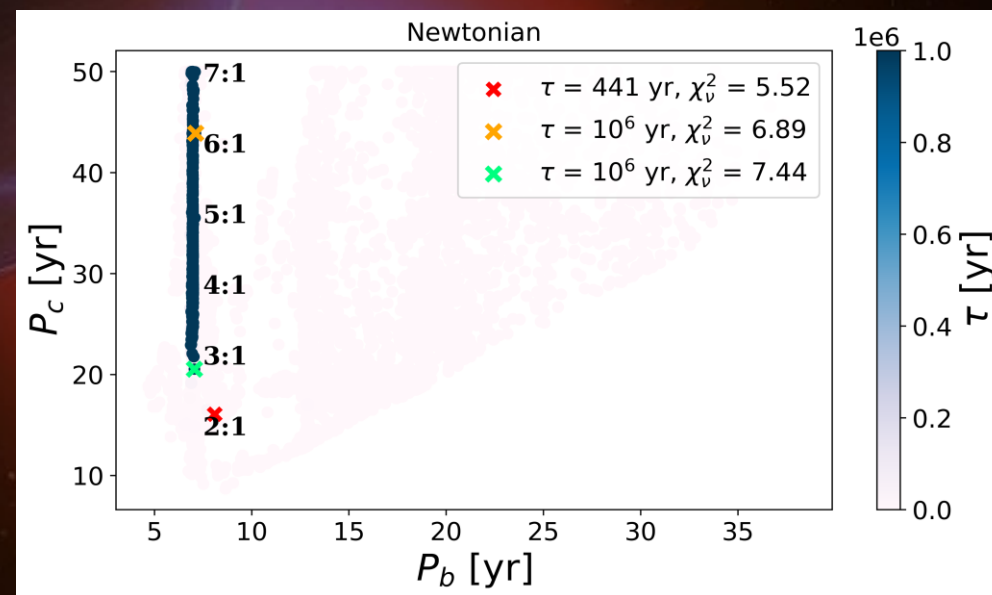
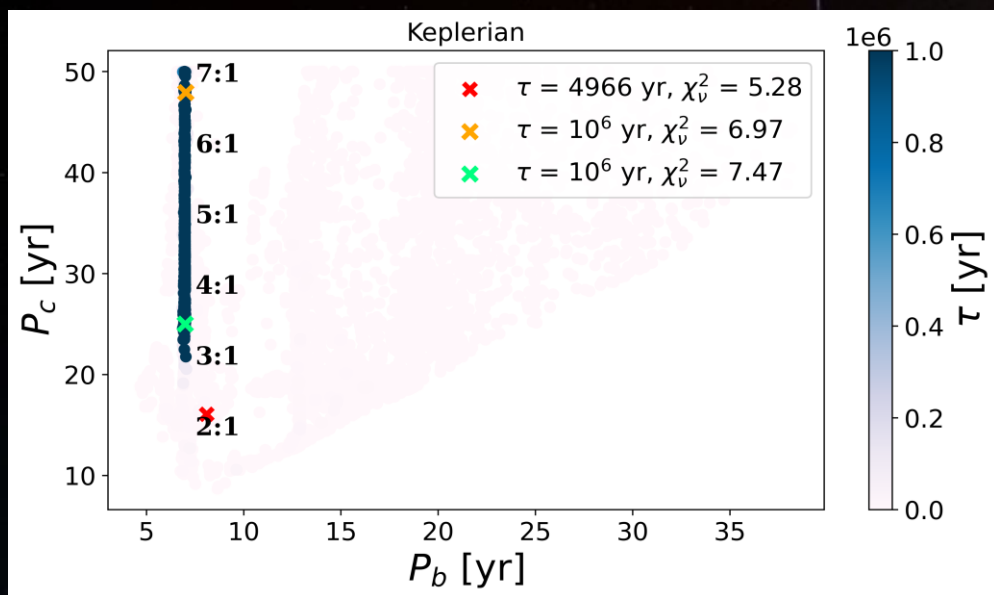
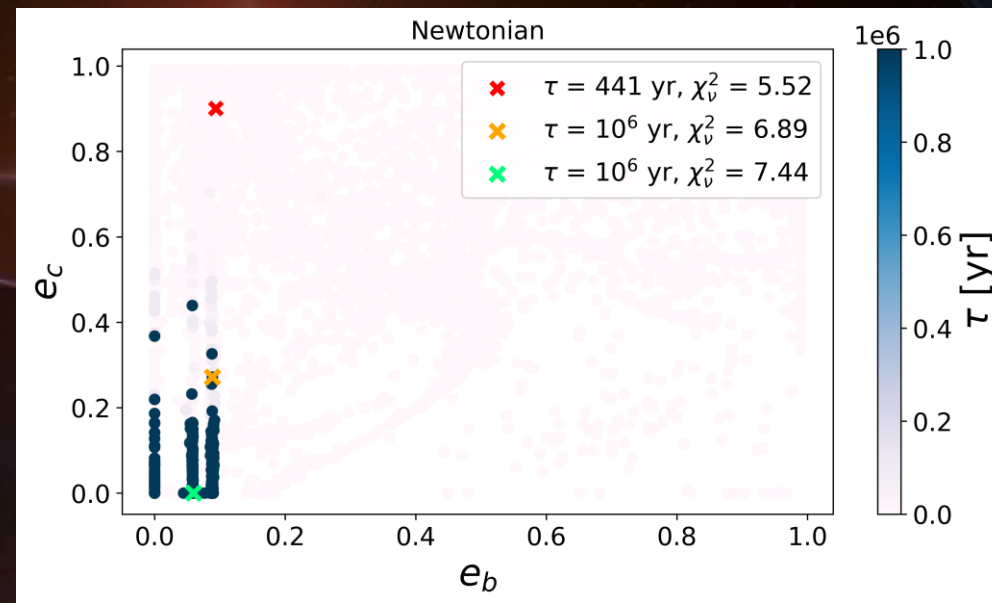
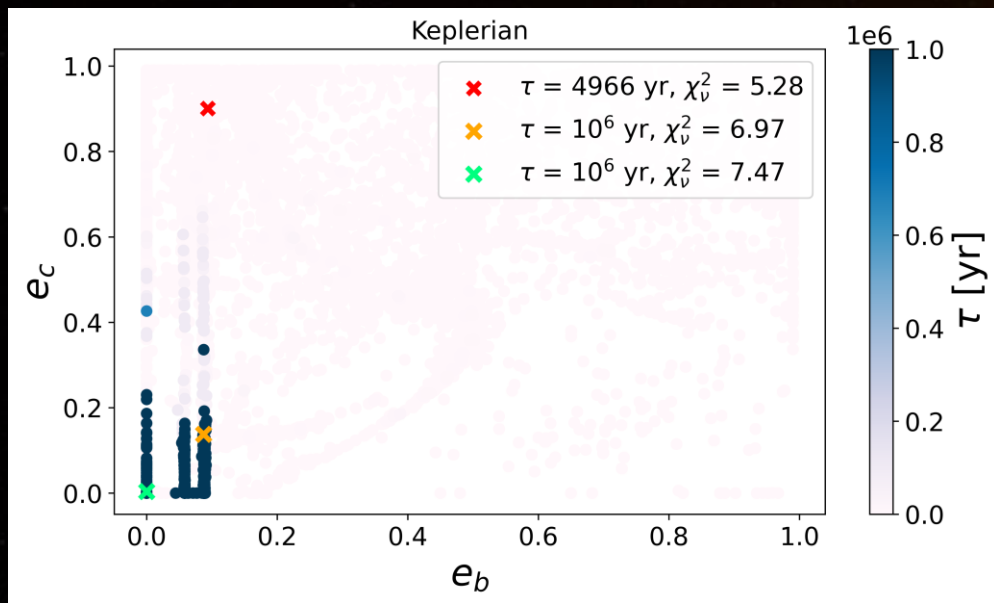


NSVS 14256825: Dataset A (Run 2) – ETV Keplerian & Newtonian fits

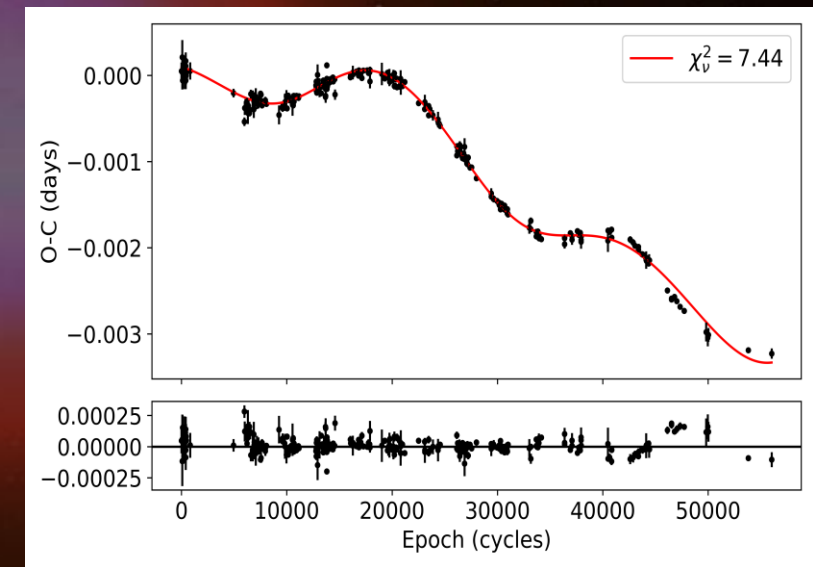
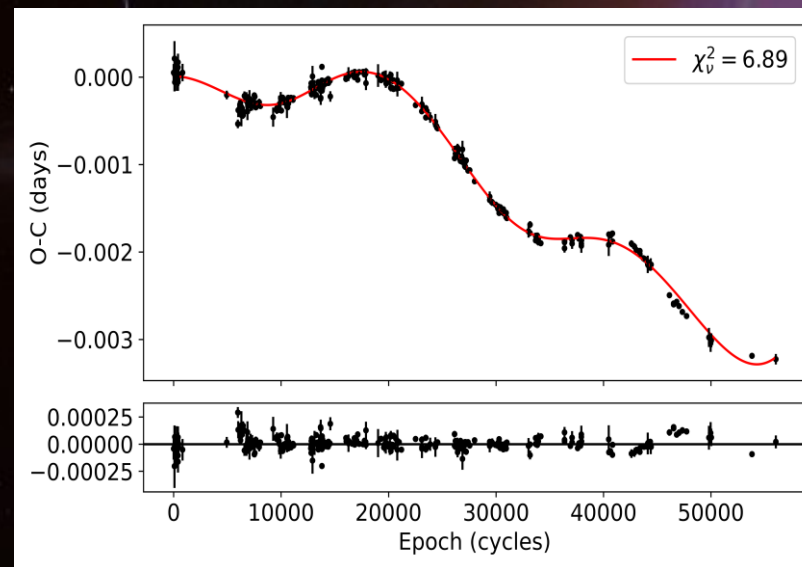
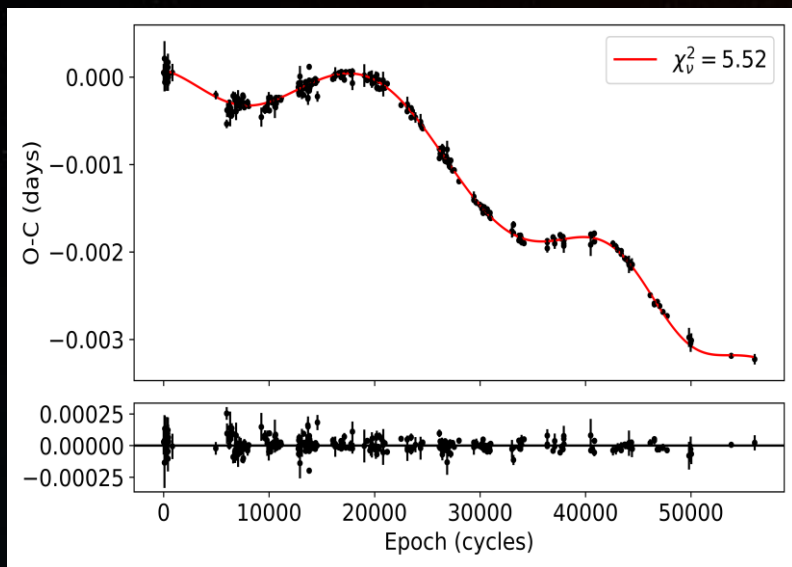
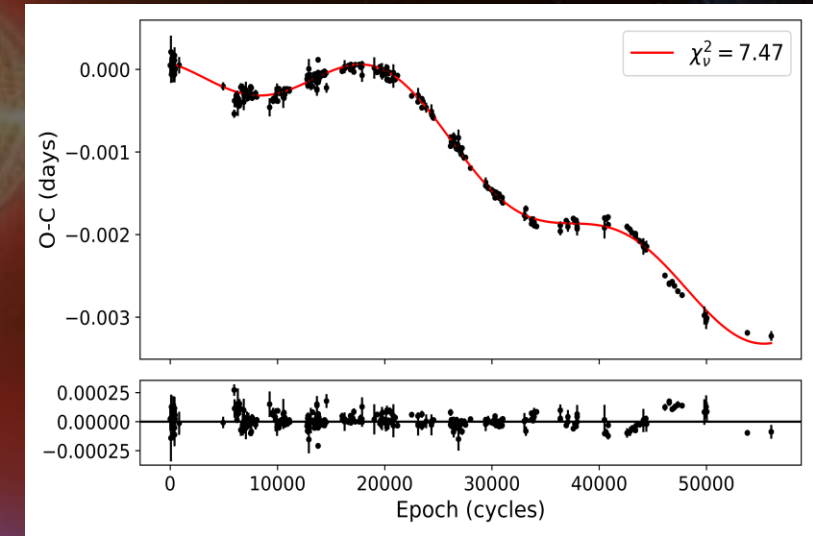
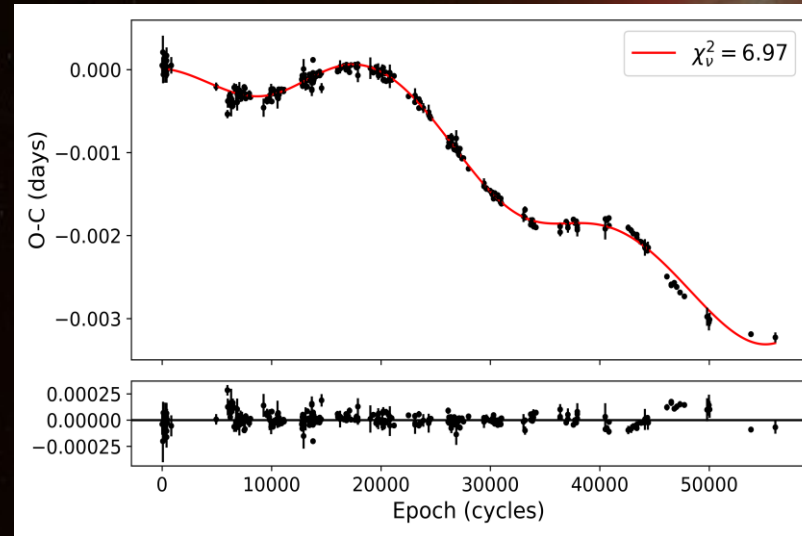
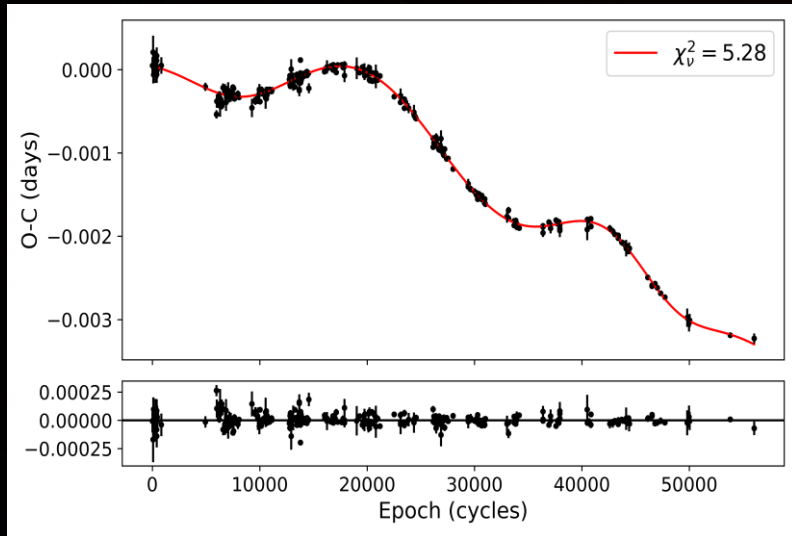


NSVS 14256825: **Dataset B (Run 2)** - lifetime distributions (colormaps)

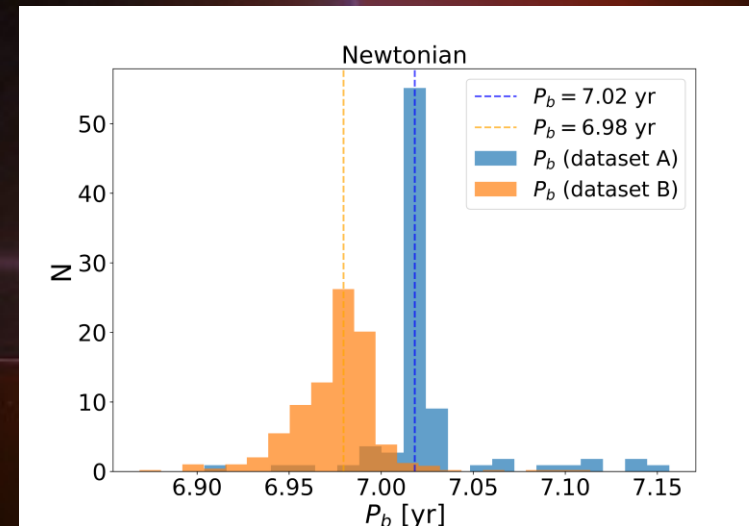
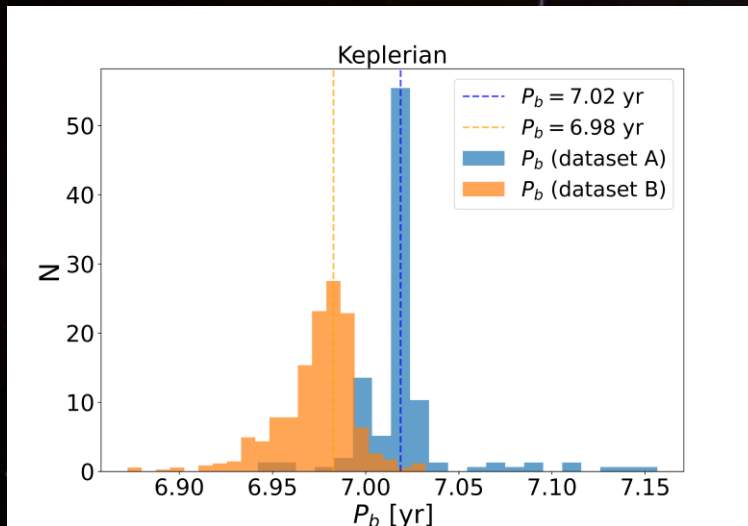
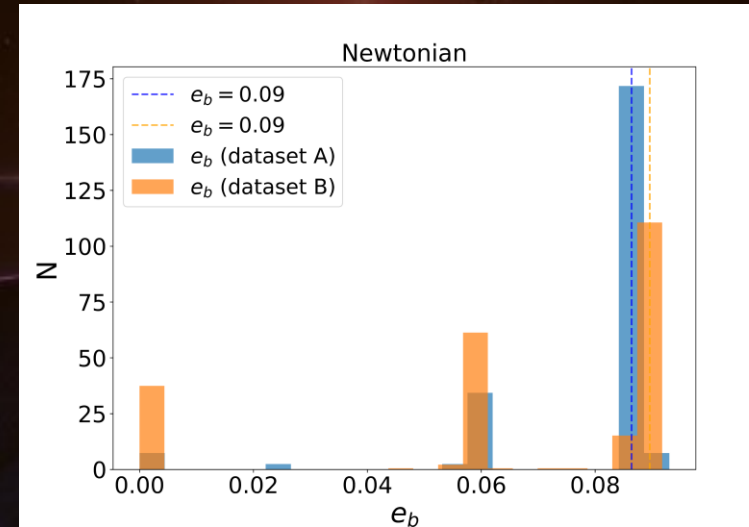
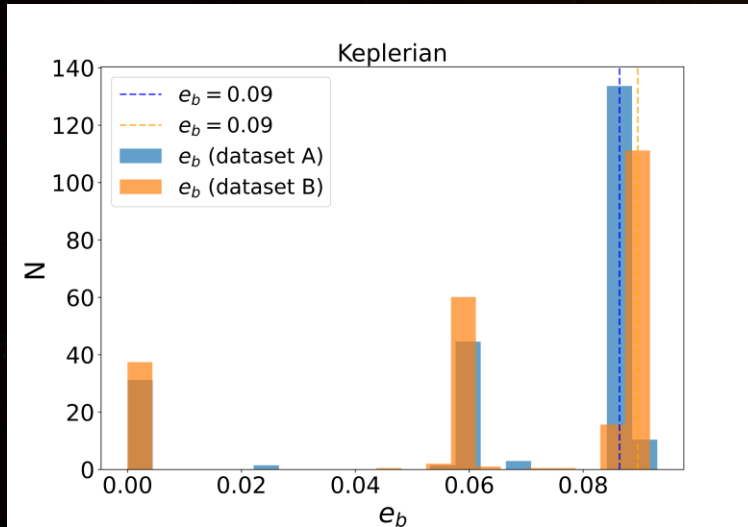
454 stable Keplerian orbits and 423 stable Newtonian orbits (8216 models)



NSVS 14256825: Dataset B (Run 2) - ETV Keplerian & Newtonian fits

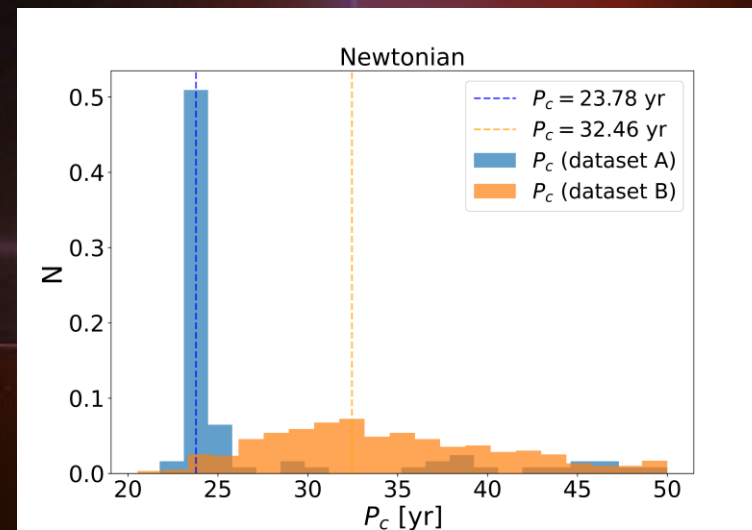
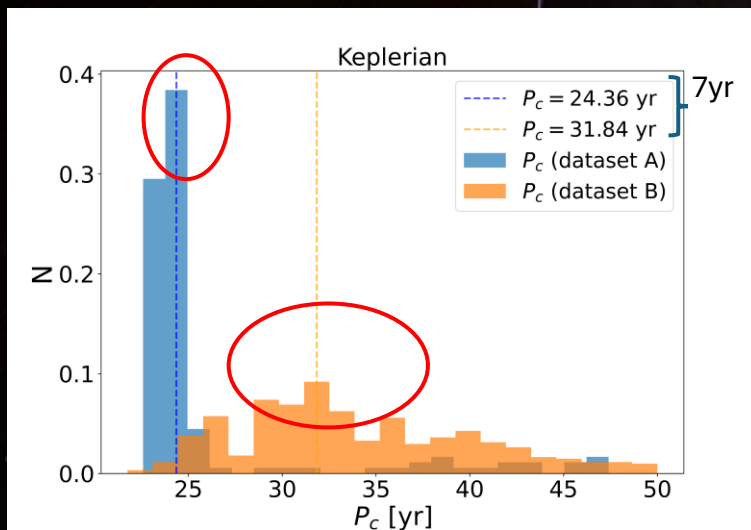
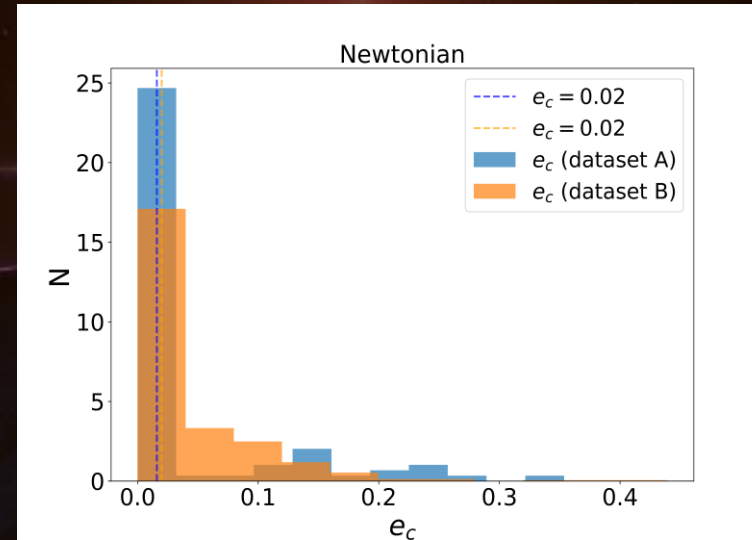
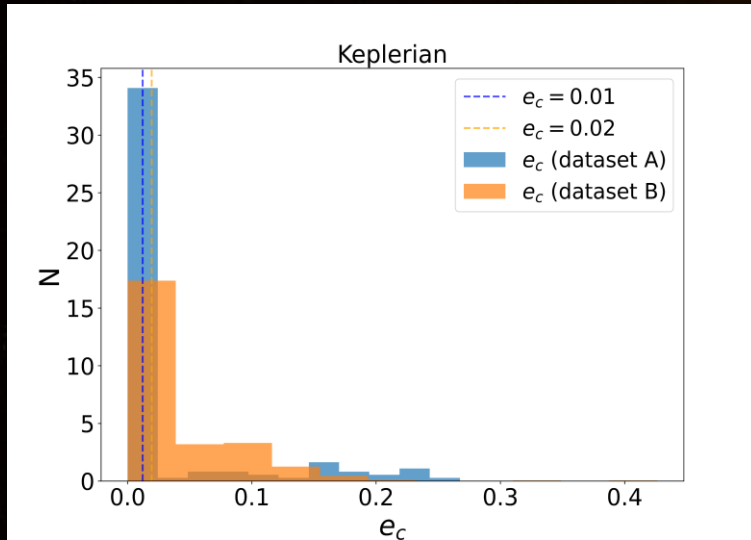


NSVS 14256825: Optimization Run 2 – Histograms of inner exoplanet



Both datasets seem to constrain the inner planet to a nearly circular orbit with a mean period of P_b 7 yr

NSVS 14256825: Optimization Run 2 – Histograms of outer exoplanet



NSVS 14256825: ($\chi^2_{min}, \chi^2_{max}$) Keplerian solutions

Table 3: Grid search optimization results of Keplerian two-planet LTTE fit after Run 2 of the fitting process for both datasets A,B.

Parameter	Dataset A (Run 2)			Dataset B (Run 2)		
	$\chi^2_{v,best}$	$\chi^2_{v,min}$	$\chi^2_{v,max}$	$\chi^2_{v,best}$	$\chi^2_{v,min}$	$\chi^2_{v,max}$
e_b	0.09(2)	0.09(3)	0.06(4)	0.09(2)	0.09(2)	0.00(1)
K_b (d)	0.00046(5)	0.00034(2)	0.00034(2)	0.00047(7)	0.00035(4)	0.00034(4)
ω_b (rad)	5.58(3)	5.34(4)	0.00(6)	5.64(5)	5.53(5)	3.33(6)
P_b (yr)	8.09(4)	6.97(5)	7.02(6)	8.10(6)	7.02(5)	6.99(04)
T_b (BJD-2400000)	55366.53(12.34)	58096.21(45.32)	55841.14(22.37)	55386.28(33.22)	58092.21(40.72)	57189.16(32.47)
e_c	0.89(3)	0.15(3)	0.0(5)	0.90(2)	0.14(3)	0.00(3)
K_c (d)	0.00056(4)	0.00093(5)	0.00507(2)	0.00054(4)	0.00679(9)	0.00096(6)
ω_c (rad)	4.61(8)	0.00(58)	6.04(9)	4.45(8)	5.06(22)	2.78(9)
P_c (yr)	16.25(5)	22.64(5)	47.40(8)	16.07(7)	47.91(28)	25.00(35)
T_c (BJD-2400000)	59660.53(10.42)	45591.75(83.24)	48715.53(112.27)	53749.47(22.41)	45174.62(115.43)	48319.52(108.45)
P_{bin} (d)	0.11037410(2)	0.11037413(3)	0.11037426(3)	0.11037410(2)	0.11037432(6)	0.11037413(3)
T_0 (BJD-2400000)	54274.20840(6)	54274.20814(9)	54274.20353(8)	54274.20847(5)	54274.20155(6)	54274.20807(4)
m_b (M_{Jup})	12.36	10.05	10.11	9.53	10.23	12.19
m_c (M_{Jup})	9.41	12.72	43.90	12.57	59.64	9.95
χ^2_v	5.20	7.02	7.97	5.28	6.97	7.47

Notes. Columns $\chi^2_{v,best}$ display the best-fitting curve parameters whereas columns $\chi^2_{v,min}$ and $\chi^2_{v,max}$ contain parameters corresponding to the minimum and maximum reduced chi-square values of stable configurations respectively. Digits in parentheses are for the uncertainty at the last significant place.

NSVS 14256825: ($\chi^2_{min}, \chi^2_{max}$) Newtonian solutions

Table 5: Self-consistent Newtonian two-planet orbital fits initialized from the results of optimization Run 2 for both datasets A,B.

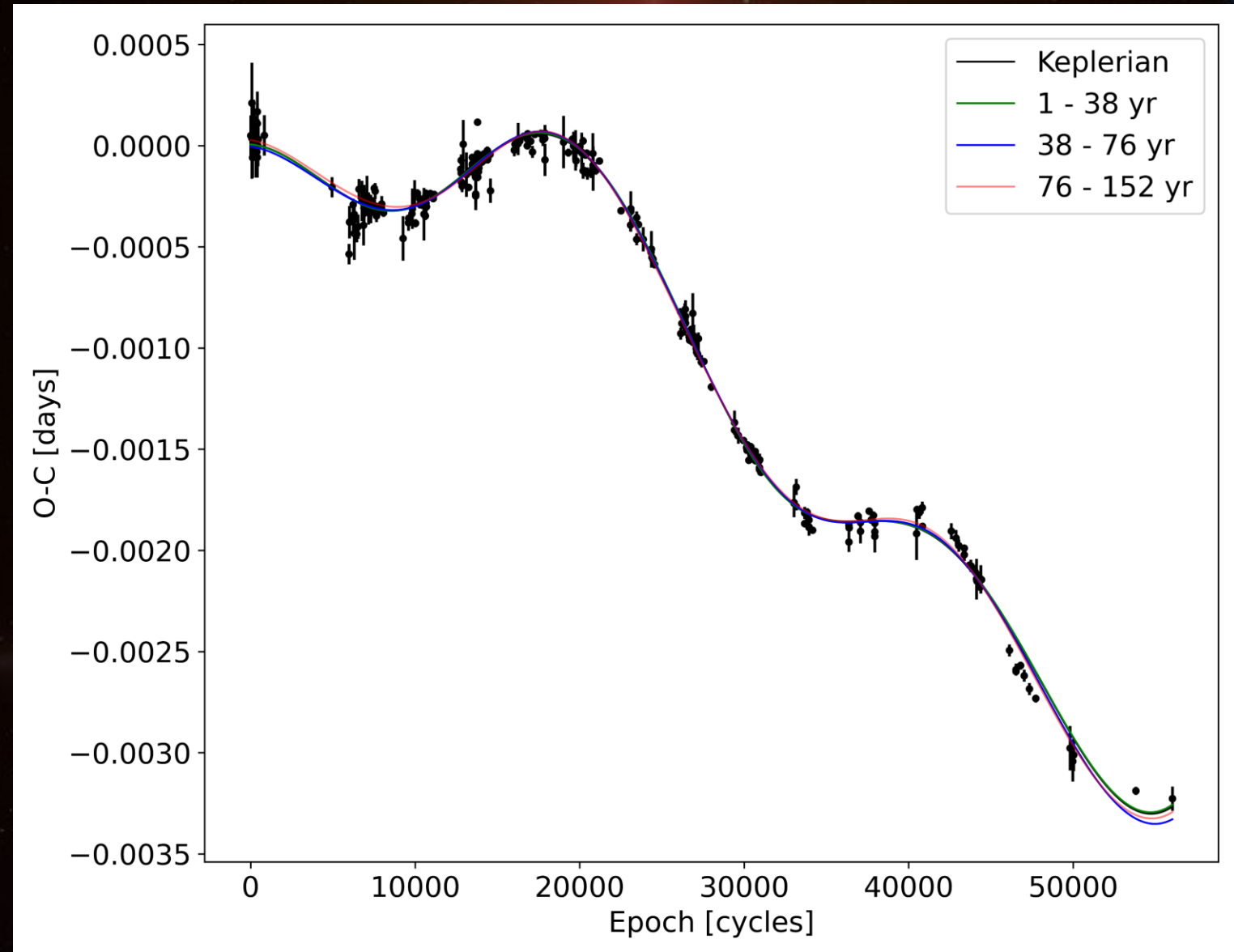
Parameter	Dataset A (Run 2)			Dataset B (Run 2)		
	$\chi^2_{v,best}$	$\chi^2_{v,min}$	$\chi^2_{v,max}$	$\chi^2_{v,best}$	$\chi^2_{v,min}$	$\chi^2_{v,max}$
e_b	0.09(3)	0.08(4)	0.06(4)	0.09(3)	0.10(4)	0.06(3)
K_b (d)	0.00046(3)	0.00034(3)	0.00035(4)	0.00047(3)	0.00036(5)	0.00034(6)
ω_b (rad)	5.56(6)	5.45(4)	6.18(3)	5.63(4)	5.46(7)	6.21(4)
P_b (yr)	8.14(4)	7.06(5)	7.07(4)	8.13(5)	6.99(7)	7.04(6)
M_b (rad)	5.42(7)	5.91(6)	6.03(6)	4.59(6)	3.22(7)	6.06(4)
e_c	0.91(4)	0.13(5)	0.17(4)	0.91(5)	0.33(5)	0.10(6)
K_c (d)	0.00058(5)	0.00091(2)	0.00530(5)	0.00058(4)	0.00714(7)	0.00067(7)
ω_c (rad)	4.65(6)	5.86(9)	5.44(5)	4.48(9)	5.20(8)	5.71(7)
P_c (yr)	16.94(4)	21.73(7)	50.45(6)	17.09(6)	41.78(7)	24.91(8)
M_c (rad)	4.21(8)	1.27(6)	0.32(8)	3.86(8)	5.30(9)	5.14(9)
P_{bin} (d)	0.11037410(2)	0.11037413(2)	0.11037426(4)	0.11037410(3)	0.11037432(5)	0.11037413(4)
T_0 (BJD-2400000)	54274.20824(4)	54274.20834(8)	54274.20294(4)	54274.20815(4)	54274.20349(7)	54274.20819(5)
m_b (M_{Jup})	12.33	10.12	10.20	12.69	10.73	11.12
m_c (M_{Jup})	9.50	12.75	44.31	9.61	70.43	8.57
χ^2_v	5.45	7.14	7.67	5.52	6.89	7.44

Notes. Columns $\chi^2_{v,best}$ display the best-fitting curve parameters whereas columns $\chi^2_{v,min}$ and $\chi^2_{v,max}$ contain parameters corresponding to the minimum and maximum reduced chi-square values of stable configurations respectively. M_b, M_c is the resulted mean anomaly of the inner and outer orbits, with each configuration being set up in the N-body osculating frame at the osculating epoch T_0 . Digits in parentheses are for the uncertainty at the last significant place.

NSVS 14256825: Test of the validity of the Keplerian fits to the data

- Investigation of orbital stability
- 8 critical solutions integrated over the lifetime of the PCEB phase of sdB binaries (100 Myr) are found stable

The LTTE effect of one indicative solution (dataset B Run 2 χ^2_{\min}) for the first 152 years phase folded in the ETV diagram



NSVS 14256825: Alternative explanations for ETV

- Can the cyclic period modulation also be driven by magnetic activity cycles of the secondary for $P_{\text{mod}}=7\text{-}48\text{yr}$? NO
- Can the spin-orbit coupling model (Applegate- Lanza) to account for residual changes in the O-C stable model fits?

Dataset A : 22 s/18 yr Dataset B : 43 s/26 yr (Lanza 2020; Mai & Mutel 2022)

$$\Delta E_{\text{rot}}/E_{\text{max}} = 0.5$$

The energy generated by the secondary star should account for the non-axisymmetric gravitational quadrupole moment ?.

Lanza 2020 : angular momentum exchange between the binary orbital motion and the spin of the magnetically active secondary. The tidal synchronization timescale $t_s = 3.4\text{-}34\text{ yr}$ similar to O-C changes.

The timescale for spin-orbit coupling may be determined by tidal synchronization instead of by magnetic activity timescales

NSVS 14256825 : Conclusions

- Hundreds of stable orbits for 2 circumbinary bodies within the 90% C.I. of $\chi_{v,best}^2$ for Keplerian and Newtonian fits with a lifetime ~ 1 Myr
- ETV can be explained by $M_b = 11M_{Jup}$ in $e_b = 0.0 - 0.09$, $P_b = 7yr$ (Constrained inner orbit) Unconstrained outer orbit with $e_c = 0.02$, $P_c = 23 (A) - 40(B)yr$ (3:1 - 7:1 MMR) for $M_c = 11 - 70M_{Jup}$
- The residuals in ETV could not be explained by a spin-orbit coupling model (Applegate -Lanza) but it may contribute. Hybrid model [HS 0705+6700 (Mai & Mutel 2022) and V471 Tau (Kundra et al. 2022)]
- Can Gaia full-epoch astrometry (~ 2025) detect the planets of ETV? YES
 $M_b = 11.12 M_{Jup}$, $P_c = 7.04$ years, $M_c = 8.57M_J$, $P_c = 24.91$
displacement of the system's barycenter $\alpha_b \sim 19$ mas, $\alpha_c \sim 34$ mas (astrometric signature)
 $d = 752.6$ pc (Gaia DR3), $G = 13.22$ mag \rightarrow scan length accuracy per optical field (Perryman et al. 2014) $\sigma_{fov} \sim 42\mu\text{as}$
- Continuously monitoring of the system for ETV data and additional observational techniques.

[2024arXiv240815358Z](https://arxiv.org/abs/2024arXiv240815358Z)